processes

Article

Analysis of the Dispersion of Viscoelastic Clusters in the Industrial Rotor-Stator Equipment

Alexander Kolomiets * and Tomas Jirout

Department of Process Engineering, Technicka 4, Faculty of Mechanical Engineering,
Czech Technical University in Prague, 16000 Prague, Czech Republic; Tomas.Jirout@fs.cvut.cz
* Correspondence: Alexander.Kolomiets@fs.cvut.cz

Abstract: Materials with complex rheology and viscoelasticity may require special equipment for processing, such as for dispergation. Rheological and mechanical data of the material can help with finding the required equipment or designing equipment. For highly viscous and complex material, a rotor-stator mixer can be a good choice for dispergation. Due to the laminar or creeping mechanism of flow inside the equipment, the dispergation mechanism is assumed to be a combination of the shear stress and slicing of the material by the rotor and stator blades. For the validation of the theory, the mechanical properties of the viscose identified in a previous work were used for comparison with the data from the CFD simulation of the rotor-stator mixer. The comparison showed that the rotor-stator device can overcome the complex shear modulus and ultimate strength of the material and homogenize the solution through a combination of the shear stress and slicing. The theory was also confirmed on the process line proposed for homogenization of the specific material. The stability of viscosity during the process of homogenization was measured and used as the main parameter for quality assessment.

Keywords: viscoelasticity; shear modulus; CFD; rheology; rotor-stator mixer

check for updates

Citation: Kolomiets, A.; Jirout, T. Analysis of the Dispersion of Viscoelastic Clusters in the Industrial Rotor-Stator Equipment. *Processes* **2021**, *9*, 2232. https://doi.org/10.3390/pr9122232

Academic Editor: Francisco J. Rubio-Hernández

Received: 16 November 2021
Accepted: 9 December 2021
Published: 11 December 2021

1. Introduction

Rotor-stator mixers are widely used in the pharmacy, food, and chemical industries, among others [1]. However, there is little information about the characteristics of these devices. Most research works use water and silicone oil for liquid–liquid dispersion [2–4]. These dispersions are almost inviscid, which leads to the turbulent regime of the flow, while the laminar regime remains unexplored. Rotor-stator mixers have a great variety of designs distinguished by the form of segments, number of slots, number of rows, etc. These devices are designed for very special conditions and materials by trial and error, so there is a lack of information about the influence of design on performance. Several research works [5–7] were focused on the influence of geometry on the performance of rotor-stator devices.

There is also a lack of information about the behavior of non-Newtonian liquids and dispersions in such mixers. Some of these liquids have a very high apparent viscosity, which can lead to a laminar regime of mixing. There are several research works about drop deformation in the laminar flow. Research by G.I. Taylor [8] showed that the drop cannot be deformed in the simple shear when the ratio of the drop's viscosity to the viscosity of the continuous phase is equal or smaller than 0.0003. If the ratio is from 0.5 to 1, there is break-up by shear forces in both machines. For ratios of 20 and above, the drop breaks in the four-roller apparatus and cannot be broken under pure shear in the parallel band apparatus. These conclusions, drawn from experimental data, were confirmed by Rumscheidt and Mason [9] and Torza et al. [10]. Windhab [11] also confirmed that high viscosity drops ($\mu_d/\mu_c \geq 4$) cannot be broken by pure shear flow.

Without pure shear stress and turbulence forces, there should be another mechanism of dispergation in the creeping flow. The homogenization of complex material by rotor-stator devices is based on the theory that the main mechanism is the combination of shear stress and slicing by the edges of the rotor and stator blades. In a previous work [12], the results of shear and slice influence with shear modulus data were calculated for specific materials. These data can be used for the validation of rotor-stator devices of different geometries for the process of mixing by using CFD simulation of mixing and analyzing shear stress on the rotor and stator surface.

2. Materials and Methods

Experiments and numerical simulations were performed with viscose of the following final composition: approximately 7–9% cellulose; 90–93% 0.8M NaOH solution; 1% modifier (by weight).

The cellulose consisted of flakes of various shapes, sizes, and dissolvent stages. The fully dissolvent flakes created a continuous phase. The continuous phase and flakes formed viscoelastic clusters of particles, which were highly inhomogeneous.

Each stage had different characteristics. Fully dissolved flakes were the final form of the product. Undissolved and half dissolved flakes needed to be prepared for better homogenization. The mechanical properties of these two stages of the material were described in a previous work [12]. The flakes showed viscoelastic behavior with a shear modulus being measured by two different techniques.

The data showed that the shear modulus value varied from 1700–16,900 Pa for 0.1 rad/s to 24,100–84,300 Pa for 100 rad/s. The dispersion of values was explained by the difference in flakes. The cut test had a slightly higher shear modulus, which can be explained by the approach taken when using the material and preparing the sample during the experiment.

The shear modulus value from the Warner–Bratzler test varied from 13,800 Pa up to 39,400 Pa with the mean value of 27,000 Pa, and the standard deviation was 7800 Pa.

The complex shear modulus was one of the two parameters needed for the comparison. One of the mechanisms of dispergation was slicing. That means that the ultimate strength of the material was also needed. Values of the ultimate strength of the viscose were obtained from the plots in the previous work and are shown in the Table 1.

Table 1. The ultimate strength of the material.

First Sample		Second Sample	
No. of Test	**Value (Pa)**	**No. of Test**	**Value (Pa)**
1	30,000	1	38,600
2	22,400	2	35,700
3	30,100	3	40,100
4	33,700	4	51,700
5	40,500	5	26,700
6	48,500	6	58,400
7	41,000	7	36,900
8		8	60,000

The mean value of the ultimate strength was 39,600 Pa with a standard deviation of 10,650 Pa. The rheological parameters of the continuous phase of the viscose were measured on the RC 20 RheoTec GmbH rheometer, with a parallel plate (ISO 6721-10, 25 mm diameter) configuration and a constant temperature of 20 °C during the measurement. The rheology parameters of the liquid phase were measured (resp. with flakes of an order of magnitude smaller than the dimension of the gap in the geometry). This measurement showed that the viscose's apparent viscosity could acquire values of tens of Pa.s.

For the the low shear rate (0.1–10 1/s), the apparent viscosity for lower shear rates was practically independent of the shear rate. For higher shear rates, viscose samples exhibited pseudoplastic behavior, i.e., the apparent viscosity decreased with an increasing shear rate. From an engineering point of view, the dependence of the apparent viscosity on the shear rate in the range of 10 ÷ 10 000 1/s can be described by a simple two-parameter power model [13].

$$\eta = K\dot{\gamma}^{n-1}, \tag{1}$$

For our model, the consistency index, *K*, was 32.826 and the power index, *n*, was 0.716. This model was used for CFD simulation.

2.1. The Equipment

2.1.1. Process Line

For the homogenization of the viscose, the process line was proposed with the rotor-stator device as the main equipment for dispergation [14] (Figure 1). It was necessary to disperse in the device—to break up the clusters of flakes and create a dispersion with a large interfacial area—for the subsequent dissolution, which took place in the next part of the process.

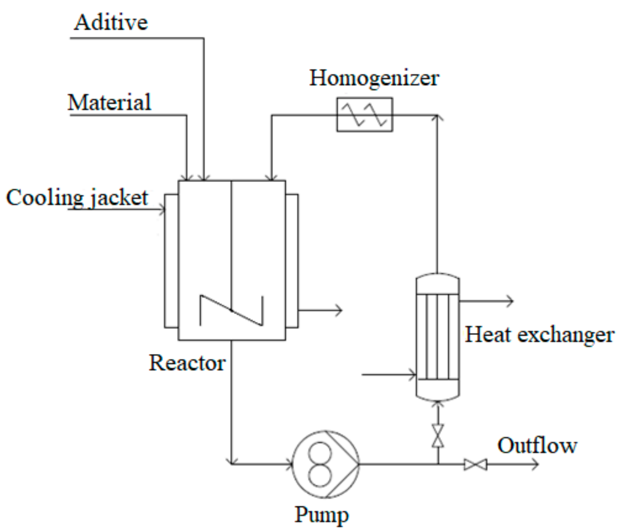

Figure 1. Proposed process line.

The alkali cellulose was fed together with the additives to the reactor, where the batch was processed. Exothermic reactions occurred in the batch, and therefore, the batch was indirectly cooled by the cooling solution flowing in the outer duplicator shell of the reactor. The batch was then pumped through a gear pump to the heat exchanger for further cooling and then pumped through an in-line rotor-stator mixer back to the reactor. Once the required batch quality was reached, it was pumped for further processing using the pump.

2.1.2. Rotor-Stator Equipment

The main part of the proposed process line was the rotor-stator mixer. The mixer needed to be capable of disrupting the flakes and dispergating them in the continuous phase. Data from rheological measurements showed that the apparent viscosity of the continuous phase could be tens of Pa.s, which led to the assumption that the regime of flow inside the mixer should be creeping. Due to lack of turbulent disruptive force, a possible mechanism of dispergation is the combination of the shear stress and slicing by rotor and stator blades. Therefore, the mixer needed to have a large number of segments with small gaps between them. For this purpose, the FHSV-B-150 M80/50 rotor-stator mixer from Lenzing Technik GmbH & Co KG, Lenzing, Austria was chosen to be a test geometry for CFD simulation of mixing (Figure 2). This was a radial in-line rotor-stator device with a total of 330 segments on the rotor and stator. The rotor consisted of 6 rows of segments, with 30 segments in each row. Two outer rows were shifted by 6 degrees to the other four. The stator consisted of 5 rows of segments, with 30 segments in each row. Two outer rows also shifted by 6 degrees to the other three. The gap between rotor and stator varied from

6.17 mm between the first (inner) rows to 0.68 mm between the last (outer) rows (Figure 3). The process parameters of the rotor-stator mixer are shown in Table 2.

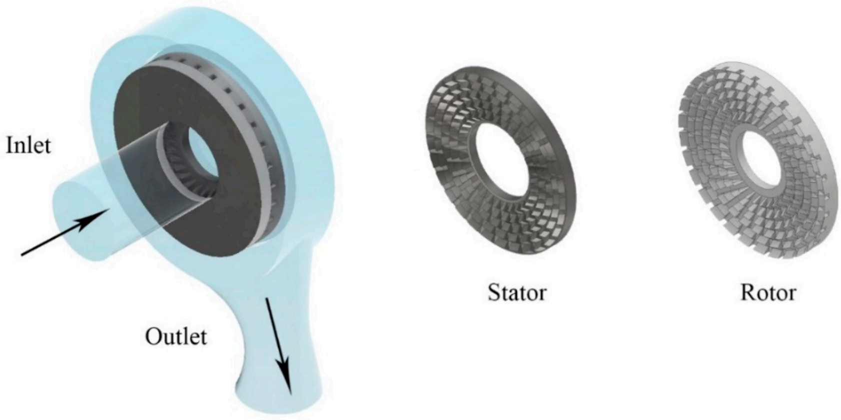

Figure 2. Model of the rotor-stator mixer.

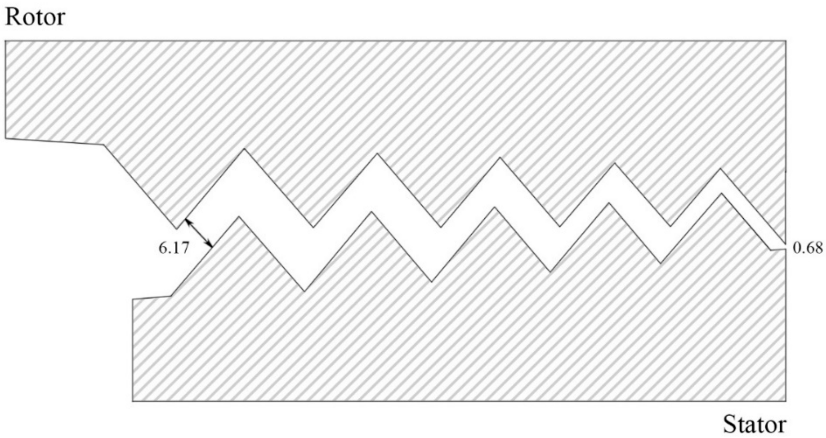

Figure 3. Cross-secton of the rotor and stator interface.

Table 2. Process parameters of the rotor-stator homogenizer.

Inlet Volume Flow	436 L/min
Outlet Pressure	0 Pa (atmoshperic)
Rotor Speed	1455 rpm
Rotor Diameter	355 mm

Based on these parameters, the Reynolds number was calculated for confirmation of the regime of mixing. The Reynolds number for the power-law model in the rotating geometry was

$$Re = \frac{N^{2-n}d^2\rho}{K}, \tag{2}$$

The density of the material was 1100 kg/m^3 and the Reynolds number was 253.3, which confirms creeping flow in the rotor-stator device.

3. CFD Simulation of Mixing Inside the Industrial Rotor-Stator

A 3D model of the mixer was created and simplified for simulation purposes. Simulation was performed using ANSYS Fluent software, version 19.2. The created mesh consisted of 2.7 mils. elements, 62% of which were concentrated in the rotor-stator interface region. Special attention was paid to the region between the rotor and stator segments where ten mesh layers were made to ensure the better quality of the velocity profile. The non-Newtonian power-law model was used for simulation and boundary conditions were used from the process parameters of the homogenizer.

Parameters of CFD Simulation

CFD simulation was performed with the following parameters: double precision, steady-state with rotating reference frame, first-order discretization, and SIMPLE pressure-velocity coupling. The under-relaxation factors and limiters for the viscosity are shown in Table 3. Surface roughness was not used in this simulation due to the fact that roughness has a negligible impact on the creeping flow.

Table 3. Under-relaxation factors and viscosity limits.

Pressure	0.3
Density	1
Body Forces	0.8
Momentum	0.5
Min Viscosity (Pa.s)	0.00001
Max Viscosity (Pa.s)	100

4. Results

4.1. CFD Simulation Results

Power output was used as a parameter for comparison with real equipment. The power output on the real equipment was 45 kW, and the numerical power output was 51 kW. A relative error of 13% showed a good agreement between actual and numerical values, which confirmed the correctness of the simulation results.

After the simulation, the values of the shear stress on the rotor and stator blades were obtained and compared with the complex shear modulus of the material (Figures 4 and 5).

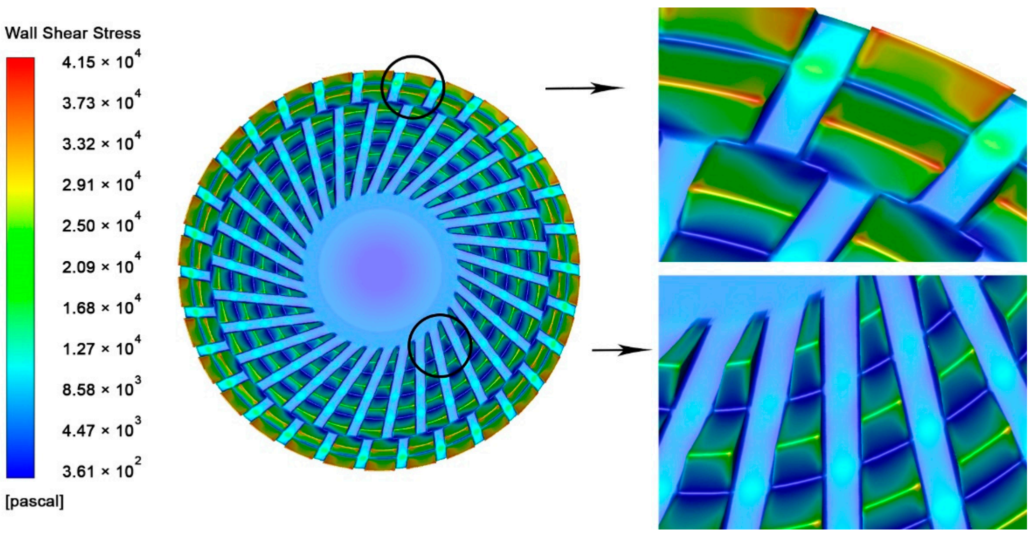

Figure 4. Shear stress on the surface of the rotor.

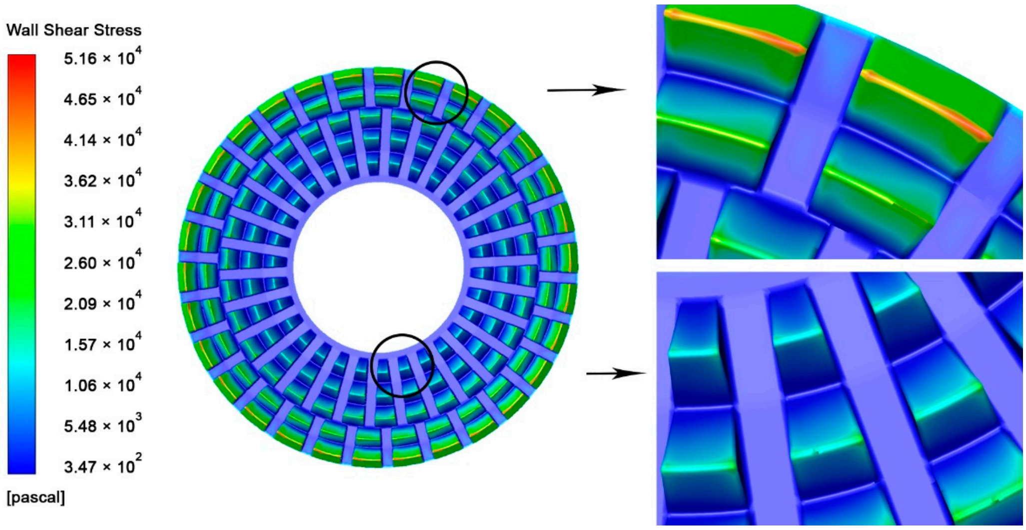

Figure 5. Shear stress on the surface of the stator.

The shear stress values from the CFD simulation had a max value of 41,500 Pa on the rotor blades (Figure 4) and 51,600 Pa on the stator blades (Figure 5). Both max values were on the tips of blades from the last rows.

Furthermore, the last rows on the stator and rotor had the largest values of shear stress on surfaces, up to 30,000 Pa. The minimum value of shear stress was 361 Pa for the rotor and 347 Pa for the stator. As was expected, the value of the shear stress increased from the center to the edge of the rotor and stator with peaks on the tips of the blades that were more involved in the slicing. The results showed that the rotor-stator mixer was capable of disrupting the viscoelastic clusters of particles. A comparison between the ultimate strength of the material and shear stress on the rotor and stator showed that the rotor-stator mixer could slice the material. A comparison with complex shear modulus showed that the rotor-stator mixer was also able to create enough shear stress for dispersion creation.

Mesh Independence Study

Three meshes were created for the purpose of the studying the independence of the mesh.

The first mesh consisted of 3.5 mil elements with just 33% of the elements concentrated in the rotor/stator region. The number of layers between the rotor and stator varied from 2 to 4 elements. The relative error in power output was 82%.

The second mesh was created with purpose of increasing the number of elements in the rotor-stator region. The mesh consisted of 1.2 mil elements with 63% of the elements concentrated in the rotor/stator region. The number of layers between the rotor and stator was 10 along the whole contact volume (Figure 3). The relative error of the power output was 13%.

The third mesh (used in the article) consisted of 2.7 mil elements with 62% of the elements concentrated in the rotor/stator region. The number of layers between the rotor and stator was the same as in the second mesh (10 layers). The relative error remained at 13%, which showed that further increasing of the mesh number was not necessary.

4.2. Confirmation of Results on the Process Line

After the simulation, the process line was installed and tested. The results from the line confirm our predictions of the ability of the rotor-stator mixing to homogenize highly viscous material with viscoelastic clusters of particles.

Viscosity was measured during normal processing time using a viscosimeter installed after the pump. Data from the process lines show increasing viscosity of the material during the process of homogenization. This phenomenon occurred due to the disruption of clusters of particles into separate smaller drops within the viscous continuous phase.

After a certain period (60 min), the viscosity was stabilized at the value 9 Pa.s (Figure 6), which means that the dispersion reached its final quality and all clusters of particles were disrupted and homogenized.

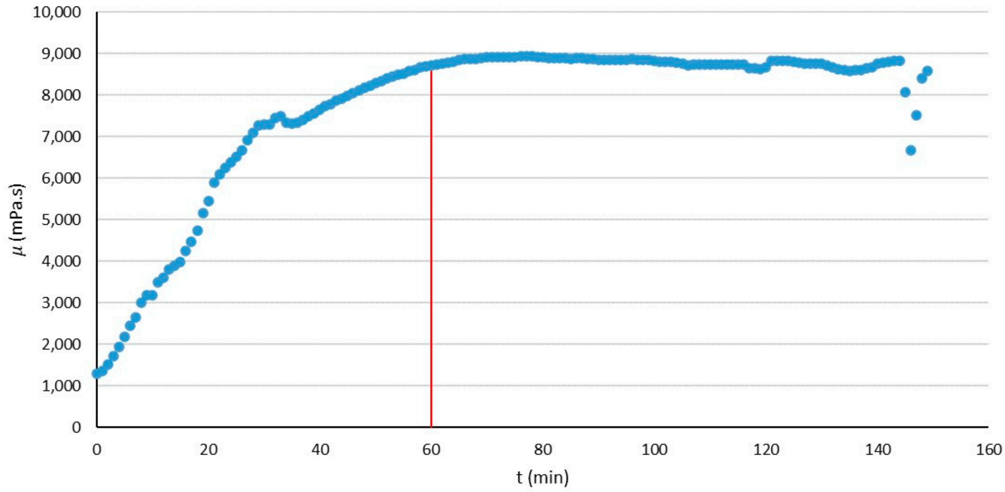

Figure 6. Viscosity during the homogenization process.

The results obtained in the preparation of the dispersion were compared with a system without a rotor-stator mixer, where the material was dispersed by a mechanical stirrer located in the reactor. After inserting a mixer of stator-rotor type in the loop (Figure 1), the whole process of preparing the dispersion was shortened by 40% compared to a system without the rotor-stator mixer. Furthermore, the technological and processing properties of the dispersion were monitored using a filtration test. These tests clearly demonstrated the achievement of a more homogeneous and fine-grained dispersion with the mixer connected to the system. Figure 6 shows an illustrative record of the measurement of the parameter used to control the process, i.e., at the moment when there was no increase in the measured apparent viscosity, the maximum possible level of dispersion was reached, the process could be stopped, and the prepared dispersion discharged into the ripening tank. The quality of the achieved dispersion was always verified using the already-mentioned filtration test.

5. Conclusions

Complex shear modulus data were taken from previous work and the rheological properties of the final stage of the material were measured. Based on this information, a new process line for material homogenization was proposed. The line consists of a tank, pump, heat exchanger, and rotor-stator mixer in the circle.

According to the existing theory, due to the laminar regime of the mixing, pure shear stress is not enough to disperse the material. A new theory focusing on the combination of shear stress with slicing as the main mechanism of dispergation was proposed. CFD simulation showed that the proposed rotor-stator geometry can generate enough shear stress on the surfaces of the rotor and stator to slice the material and disperse the viscoelastic clusters within the viscous continuous phase. Adding the rotor-stator mixer to the process line confirmed that the mixer helps in homogenization. The whole process of preparing the dispersion was shortened by 40% compared to a system without the rotor-stator mixer. The technological and processing properties of the dispersion were monitored using a filtration test. These tests clearly demonstrated the achievement of a more homogeneous and fine-grained dispersion with the mixer connected to the system.

Author Contributions: Conceptualization, T.J. and A.K.; methodology, T.J.; software A.K.; validation, T.J. and A.K.; formal analysis, A.K.; investigation A.K.; resources, T.J. and A.K.; data curation, T.J.; writing—original draft preparation, A.K.; writing—review and editing, T.J.; visualization, A.K.;

supervision, T.J.; project administration, T.J.; funding acquisition, T.J. All authors have read and agreed to the published version of the manuscript.

Funding: This work was supported within the framework of the Czech Ministry of Industry and Trade grant No. FV30284 Development of new homogenization technology high viscous dispersion of the non-newton type, and by the Grant Agency of the Czech Technical University in Prague, within the framework of grant No SGS20/119/OHK2/2T/12.

Conflicts of Interest: The authors declare no conflict of interest.

References

1. Atiemo-Obeng, V.A.; Calabrese, R.V. Rotor-Stator Mixing Devices. In *Handbook of Industrial Mixing*; Paul, E.L., Atiemo-Obeng, V.A., Kresta, S.M., Eds.; Wiley: Hoboken, NJ, USA, 2004; pp. 479–505.
2. Jasińska, M.; Bałdyga, J.; Hall, S.; Pacek, A.W. Dispersion of oil droplets in rotor–stator mixers: Experimental investigations and modeling. *Chem. Eng. Process. Process. Intensif.* **2014**, *84*, 45–53. [CrossRef]
3. Rueger, P.E.; Calabrese, R.V. Dispersion of water into oil in a rotor–stator mixer. Part 1: Drop breakup in dilute systems. *Chem. Eng. Res. Des.* **2013**, *91*, 2122–2133. [CrossRef]
4. Hall, S.; Cooke, M.; El-Hamouz, A.; Kowalski, A.J. Droplet break-up by in-line Silverson rotor–stator mixer. *Chem. Eng. Sci.* **2011**, *66*, 2068–2079. [CrossRef]
5. Mortensen, H.H.; Innings, F.; Hakansson, A. The effect of stator design on flowrate and velocity fields in a rotor-stator mixer—An experimental investigation. *Chem. Eng. Res. Des.* **2017**, *121*, 245–254. [CrossRef]
6. Mortensen, H.H.; Innings, F.; Hakansson, A. Local levels of dissipation rate of turbulent kinetic energy in a rotor-stator mixer with different stator slot widths—An experimental investigation. *Chem. Eng. Res. Des.* **2018**, *130*, 52–62. [CrossRef]
7. Utomo, A.; Baker, M.; Pacek, A.W. The effect of stator geometry on the flow pattern and energy dissipation rate in a rotor-stator mixer. *Chem. Eng. Res. Des.* **2009**, *87*, 533–542. [CrossRef]
8. Taylor, G.I. The Formation of Emulsions in Definable Fields of Flow. *Proc. Roy. Soc.* **1934**, *146*, 501–523.
9. Rumscheidt, F.D.; Mason, S.G. Particle motions in sheared suspensions. Deformation and burst of fluid drops in shear and hyperbolic flow. *J. Colloid Sci.* **1961**, *16*, 238–261. [CrossRef]
10. Torza, S.; Cox, R.G.; Mason, S.G. Particle motions in sheared suspensions. Transient and steady deformation and burst of liquid drops. *J. Colloid Interface Sci.* **1972**, *38*, 395–411. [CrossRef]
11. Windhab, E.J.; Dressler, M.; Feigl, K.; Fischer, P.; Megias-Alguacil, D. Emulsion processing—From single-drop deformation to design of complex processes and products. *Chem. Eng. Sci.* **2005**, *60*, 2101–2113. [CrossRef]
12. Kolomiets, A.; Jirout, T. An investigation of the elastic properties of viscoelastic clusters of particles: A comparison between two methods. *Polym. Eng. Sci.* **2021**, *61*, 1440–1448. [CrossRef]
13. Atiemo-Obeng, V.A.; Calabrese, R.V. *Handbook of Industrial Mixing*; Paul, E.L., Atiemo-Obeng, V.A., Kresta, S.M., Eds.; John Wiley & Sons, Inc.: Hoboken, NJ, USA, 2003. [CrossRef]
14. Jirout, T.; Kolomiets, A.; Kovač, D.; Mrázek, D. *Equipment for Dispersing Elastic or Viscoelastic Particles and Flakes in a Viscous Liquid Phase*; Czech Utility Model No. 34 485; Industrial Property Office of the Czech Republic: Prague, Czech Republic, 2020.